arXiv:0909.5231v1 [quant-ph] 29 Sep 2009

Entanglement and localization of the one spin excitation states in a quantum XX chain with a impurity

A. Zwick* and Omar Osenda†

Facultad de Matemática, Astronomía y Física,
Universidad Nacional de Córdoba, Córdoba, Argentina and
IFFAMAF-CONICET

(Dated: September 29, 2009)

Abstract

One spin excitation states are involved in the transmission of quantum states and entanglement through a quantum spin chain, the localization properties of these states are crucial to achieve the transfer of information from one extreme of the chain to the other. We investigate the bipartite entanglement and localization of the one excitation states in a quantum XX chain with one impurity. The bipartite entanglement is obtained using the Concurrence and the localization is analyzed using the inverse participation ratio. Changing the strength of the exchange coupling of the impurity allows us to control the number of localized or extended states. Our results show that equally localized states do not possess the same bipartite entanglement and suggest that only a restricted class of localizated states allows the storage and transmission of quantum states.

PACS numbers: 75.10.Pq; 03.67.Hk; 03.67.Mn; 05.50.+q

---

*Electronic address: zwick@famaf.unc.edu.ar

†Electronic address: osenda@famaf.unc.edu.ar

I. INTRODUCTION

Since the first works dealing with the entanglement shared by pairs of spins on a quantum chain, the translational invariance of the chain (and its states) has been exploited to facilitate the analysis of the problem [1, 2, 3]. Anyway, there is a number of problems which do not possess the property of being translationally invariant: semi-infinite chains, chains with impurities [4] or, in a more abstract sense, random quantum states [5]. These problems have localized quantum states whose properties strongly differ from those of translationally invariant quantum states.

Localized quantum states can be used to storage quantum information [6] an play and important role in the propagation of entanglement through a quantum spin chain [7]. This kind of states also appears in some models of quantum computers in presence of static disorder [8].

Since the localization of a quantum state is a global property it seems natural to study its properties using a global entanglement measure as, for example, the one proposed by Meyer and Wallach [9]. Giraud *et al.* [10] derived exact expressions for the mean value of the Meyer-Wallach entanglement for localized random vectors and studied the dependence of this measure with the localization length of the states. Viola and Brown [11] studied the relationship between generalized entanglement and the delocalization of pure quantum states. Of course there are other possibilities to study the relationship between localization of quantum states and entanglement. The bipartite entanglement and localization of one-particle states in the Harper model has been addressed by Li *et al.* [12], the entanglement entropy at localization transitions is studied in reference [13] and the localized entanglement in one-dimensional Anderson model in reference [14].

In many proposals of quantum computers the qubit energies can be often individually controlled, this corresponds to controllable disorder of a spin system. Besides, in these models, the effective spin-spin interaction is usually strongly anisotropic, it varies from the Ising coupling in nuclear magnetic resonance and other systems [15] to the XY-type or the XXZ-type coupling in some Josephson-junction-based systems [16]. The localization properties of one and two excitation states in the XXZ spin chain with a defect was studied with some detail by Santos and Dykman [17], but they did not study the entanglement of the one and two excitation states.

In this paper we are interested in the behavior of the localization and the bipartite entanglement of the pure eigenstates of a quantum chain with one impurity when the localized state, produced by the presence of the impurity, enters in the band of one magnon states [17], or one spin excitation states. The one spin magnons are extended states [17]. Our motivation to examine this problem is twofold.

First, we aim to characterize the transition between a localized pure state and a delocalized state when this transition is driven by the intensity of the interaction of the impurity with the rest of the chain. Our results show that when the localized state enters the band of extended states the localization and bipartite entanglement of all the states in the band changes. For a vector Ψ in an N-dimensional Hilbert space, localization can be quantified through the inverse participation ratio (IPR) $L_{IPR} = \sum_i |\Psi_i|^2 / \sum_i |\Psi_i|^4$ where Ψ_i are the components of Ψ.

Second, recently Ferrón *et al.* [18] studied the entanglement of a resonance state in a quantum dot, the resonance state appears when the ground state of two electrons confined in the quantum dot (the localized state) is no longer stable and enters the continuum of (delocalized extended) states above the ionization threshold. The eigenfunctions of the quantum dot above the threshold show a peculiar behavior: if $S_i(R)$ is the entanglement of the $i - th$ energy level, $S_i^m(R_i^m)$ is the minimum value of $S_i(R)$ as a function of R (R is the radius of the quantum dot), *i.e.* R_i^m is where $S_i(R)$ attains its minimum, then $R_1^m > R_2^m > R_3^m > \ldots$. Our results show that a very similar scenario is shown by the eigenstates of the quantum chain, in particular our results show that the ordering of the entanglement of the different eigenstates follows closely the ordering dictated by the amount of localization of the quantum state.

The paper is organized as follows, in Section II we present the XX model describing the quantum spin chain with a impurity, and briefly describe how to solve it. In Section III we analyze in some detail the spectrum of the one spin excitations. In Section IV we present the results obtained for the inverse participation ratio for each one spin excitation eigenstate while the bipartite entanglement of the eigenstates is analyzed in Section IV. Finally, in Section V, we discuss some of the implications of our results for the transference of states through the chain.

II. THE MODEL

We consider a linear chain of N-qubits with XX interaction, in an external magnetic field. The coupling intensities are homogeneous except at one site where the coupling is different. The system is described by the Hamiltonian

$$H_{xy}(\alpha) = \alpha J(\sigma_1^x\sigma_2^x + \sigma_1^y\sigma_2^y) + \sum_{i>1} J(\sigma_i^x\sigma_{i+1}^x + \sigma_i^y\sigma_{i+1}^y) - h\sum_i \sigma_i^z \qquad (1)$$

where σ^γ are the Pauli matrices, $h > 0$ is the external field, $J < 0$ is the exchange coupling coefficient and αJ is the impurity exchange coefficient, $\alpha = 1$ corresponds to the homogeneous case.

Since the Hamiltonian commutes with $S_z = \Sigma_i\sigma_i^z$, the total Hilbert space can be expressed as a sum over subspaces characterized by the number of excited spins in the chain. We study the eigenvectors in the one excitation subspace. The basis set for this subspace is denoted by $|n\rangle = (\uparrow\uparrow \ldots \uparrow\downarrow_n\uparrow \ldots \uparrow)$, where $n = 1, \ldots, N$, *i.e.* the basis set size is equal to the number of spins of the chain.

In the one excitation basis, the Hamiltonian H is represented by a $N \times N$ matrix

$$\mathcal{H} = \begin{pmatrix} h & \alpha J & 0 & \ldots & 0 \\ \alpha J & h & J & \ldots & 0 \\ 0 & J & h & \ldots & 0 \\ \vdots & \vdots & \vdots & \ddots & J \\ 0 & 0 & 0 & J & h \end{pmatrix} \qquad (2)$$

The Hamiltonian, Eq. (1) can be solved exactly using the non-interacting particle representation given by the *Wigner-Jordan Transformation*, which maps the spin system into a spin-less fermion system [19]. However. we solve the eigenvalue problem $\mathcal{H}\mathbf{c}_i = E_i\mathbf{c}_i$ numerically. The eigenvalues E_i and the eigenvectors $\mathbf{c}_i$ allow us to construct all the relevant physical quantities.

III. ENERGY SPECTRUM

The one excitation spectrum consists of N eigen-energies, denoted by $\{E_1 \leq E_2 \leq \ldots \leq E_N\}$. Choosing the total number of spins even, and substracting a constant that depends on h, the spectrum results symmetrical with respect to zero ($E = 0$ is not an eigenvalue) for any value of α. Then $\{E_1, ..., E_M\}$ are negative values whereas $\{E_{M+1}, ..., E_N\}$ are positive, where $M = N/2$. In the homogeneous case ($\alpha = \alpha_J \equiv 1$), the energy spectrum lies between the values $\pm 2|J|$. The size of the chain only changes the number of eigenvalues between those extreme values, becoming a continuous spectrum when $N \to \infty$.

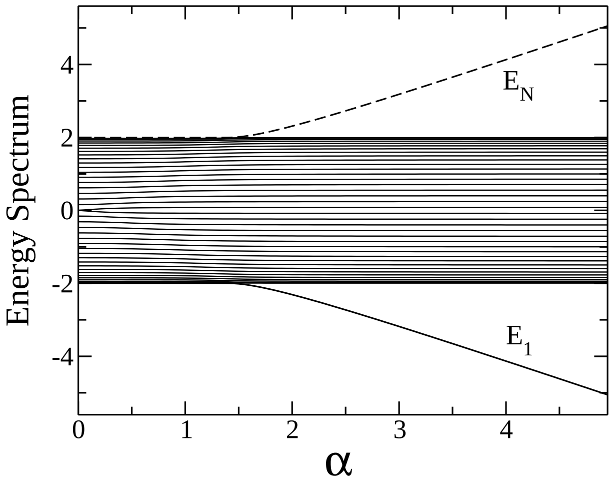

FIG. 1: The one excitation spectrum *vs* α for a spin chain with 40 spins. For α large enough the spectrum shows two isolated eigen-energies and one band $|E| \leq 2|J|$. The two isolated curves correspond to the minimal eigen-energy E_1 (continuous line) and the maximal eigen-energy E_N (dashed). At the critical value α_c the isolated energies go into the band causing a slight distortion on the behaviour of energies inside the band. In this figure we use $|J| = 1$.

The inhomogeneous case shows a different behavior. For large enough α the minimal and the maximal eigen-energy become isolated from the band. There is a critical value α_c which separates the region of the spectrum where the energies make a band ($0 < \alpha < \alpha_c$) from the region where the energies make a band with two energies isolated ($\alpha > \alpha_c$). When α grows large enough the minimal and maximal energies move apart from the band changing proportionally to $-\alpha$ and $+\alpha$, respectively. This behavior is depicted in Fig.1.

As can be seen from Figure 1 most of the eigen-energies seem to be fairly independent of α, except for the minimal and maximal energies. Further insight about the behavior of a given energy can be obtained studying its derivative with respect to α.

The value of α that separates the region where the minimal eigenvalue is isolated from the

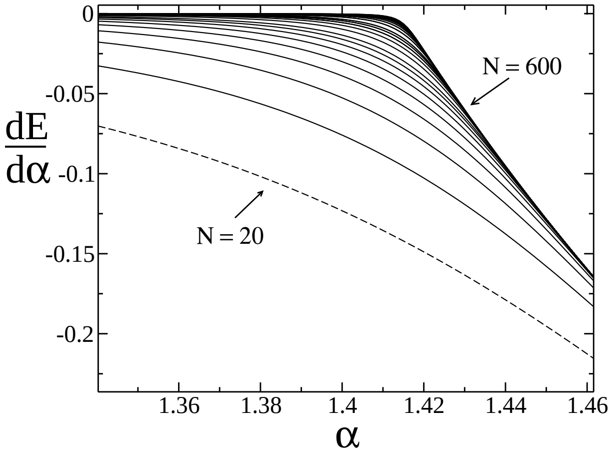

FIG. 2: $dE_1/d\alpha$ *vs* α for different lenghts of the spin chain, from bottom to top, N= 20, 30,..., 100, 120,..., 200, 250, .., 600.

region where the minimal eigenvalue belongs to the band depends on N. Roughly speaking, $\alpha_c(N)$ is the larger value of α such that $\frac{dE_1}{d\alpha} = 0$ for a chain of N spins. When $N \to \infty$ the critical value $\alpha_c(N)$ becomes independent of N. Figure 2 shows the behavior of $\frac{dE_1}{d\alpha}$ for several values of N. For N large enough $\frac{dE_1}{d\alpha} = 0$ for $\alpha \lesssim \alpha_c \simeq \sqrt{2}$. As we will show, there are other ways to detect when the minimal eigenvalue belongs to the band or is isolated. In the rest of the paper we use $N \geqslant 40$, and $\alpha_c = \lim_{N\to\infty} \alpha_c(N)$. The maximal eigen-energy behaves similarly to the minimal eigen-energy so we do not present results about depends on the chain size.

The behavior of the eigen-energies that are neither the minimal or the maximal is a bit more complex. There are to regimes in which the derivative of an eigen-energy is noticeable: i) for $\alpha \lesssim \alpha_c$ there is a number of avoided crossings between successive eigen-energies, because of the "collision" among the minimal (or maximal) eigen-energy and the band; ii) near $\alpha = 0$ there are two eigen-energies that become degenerate. The system changes from a chain with N coupled spins to a chain with $N-1$ coupled spins and an uncoupled spin that is affected by the external field. These two regimes are depicted in Figure 3. Outside the regions in which these regimes are observable, the derivative of any eigen-energy with respect to α is basically zero. In other words two given eigen-energies $E_i(\alpha)$ and $E_{i+1}(\alpha)$ are, basically, two horizontal parallel lines, except in: i) a small region of α in which they present an avoided crossing; ii) the region near $\alpha \to 0$.

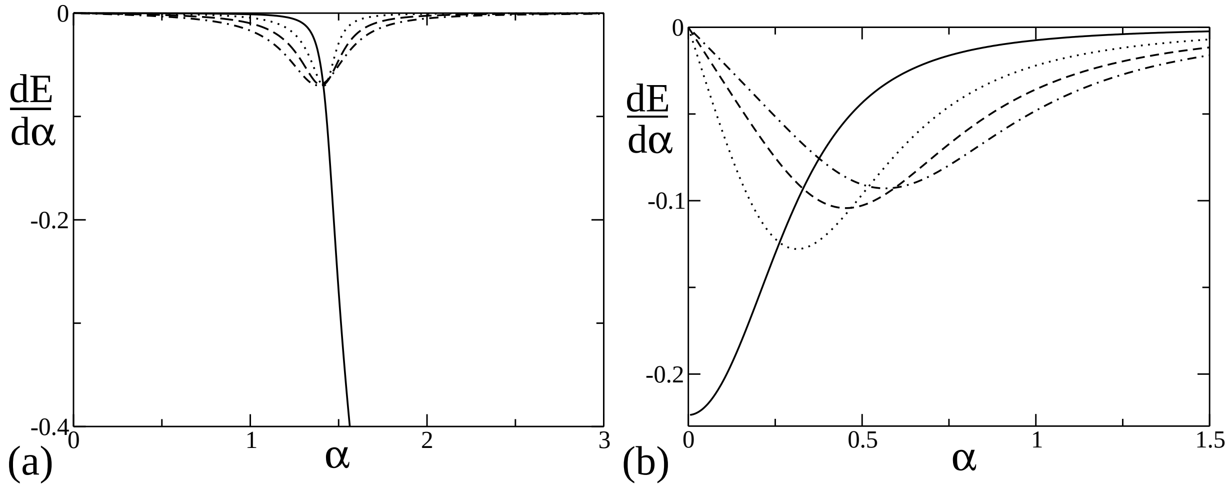

FIG. 3: (a) Behavior of $dE_i/d\alpha$ for the first four eigenvalues in the region near α_c. The continuous line corresponds to the derivative of E_1, the dotted to E_2, the dashed to E_3, and the dot-dashed to E_4. The derivative of E_1 approaches zero when the eigenvalue enters into the band. The small valleys in the derivatives of E_1, E_2 and E_3 shown that these eigenvalues are non-increasing functions of α. When the derivative of the eigenvalues is nearly zero the distance between successive eigenvalues remains constant, but when the derivative is different from zero two successive eigenvalues tend to be closer, presenting an avoided crossing. (b) $dE_i/d\alpha$ *vs* α, for $i = M = N/2$ (continuous line) ,$M-1$ (dotted), $M-2$ (dashed), and $M-3$ (dashed-dotted). The spin chain has $N = 40$. The eigen-energies are non-increasing functions of α, $dE_i/d\alpha \leq 0, \forall \alpha$.

The eigenstates in the one excitation subspace $|\Psi_E(\alpha)\rangle$ are given by

$$H(\alpha)|\Psi_E(\alpha)\rangle = E|\Psi_E(\alpha)\rangle. \tag{3}$$

The one excitation eigen-states can be written as an expansion in the one excitation basis set

$$|\Psi_E(\alpha)\rangle = \sum_{n=1}^{2N} c_n(E,\alpha)\,|n\rangle\,, \tag{4}$$

where the coeficcients $c_n(E,\alpha)$ contain all the information concerning the localization and entanglement properties of the eigenstates. The coefficients $c_n(E,\alpha)$ can be written as [17]

$$c_n(E,\alpha) = de^{i\theta n} + d'e^{-i\theta n}. \tag{5}$$

We will use the expression in Eq. 5 to analyze some of our numerical results.

The density matrix for each eigenstate is given by

$$\hat{\rho}_E(\alpha) = |\Psi_E(\alpha)\rangle\langle\Psi_E(\alpha)|, \tag{6}$$

which is a $N \times N$ matrix in the one excitation subspace.

IV. LOCALIZATION OF THE EIGEN-STATES

The localization of the eigen-states can be measured trough the inverse participation radio (IPR) [10],

$$L_{IPR}(|\Psi\rangle) = \frac{\sum_i \Psi_i^2}{\sum_i \Psi_i^4}, \tag{7}$$

where Ψ_i are the components of $|\Psi\rangle$, which is a vector of a D-dimensional Hilbert space. The minimum value in this measure is 1 when the state is highly localized (*i.e.*, when Ψ_i is nonzero for only one particular value of i), and the maximum value is D when the state is uniformly distributed (ie., when $\Psi_i = 1/\sqrt{D}$ for all i).

We are considering the one excitation eigenstates $\Psi_i = c_i(E,\alpha)$, where the $c_i(E,\alpha)$ are the coefficientes of Equation 4. Figure 4 shows the inverse participation ratio L_{IPR} of several eigenstates $\{|\Psi_{E_1}\rangle, ..., |\Psi_{E_N}\rangle\}$ as a function of the impurity coupling α . Two states with symmetrical eigen-energies with respect to zero, say $|\Psi_{E_j}\rangle$ and $|\Psi_{E_{N-j+1}}\rangle$ where $j \leq N/2$, have the same IPR. For these two eigenstates we get that

$$|\Psi_{E_j}\rangle = \sum_i \Psi_i^{(j)}|i\rangle, \qquad |\Psi_{E_{N-j+1}}\rangle = \sum_i \Psi_i^{(N-j+1)}|i\rangle, \tag{8}$$

with

$$\Psi_i^{(j)} = cte \times (-1)^i \Psi_i^{(N-j+1)}, \quad cte = \pm 1, \tag{9}$$

from this relationship it is easy to obtain that $L_{IPR}(|\Psi_{E_j}\rangle) = L_{IPR}(|\Psi_{E_{N+1-j}}\rangle)$. As a consequence, each curve in Figure 4 is double.

We call a state $|\Psi\rangle$ *extended* if $L_{IPR}(|\Psi\rangle) \sim O(N)$, *i.e.* when the inverse participation ratio is of same order than the length of the chain.

There are three regions where the behaviour of the L_{IPR} is qualitatively different. These regions are separated by α_J and α_c, for these two values of α all the eigenstates are equally localized.

The interval $0 < \alpha < \alpha_J$ shows several localized eigenstates corresponding to energies close to zero. Calling $\alpha^m_{E_i}$ the value of α such that $L_{IPR}(E_i,\alpha) = L_{IPR}(|\Psi_{E_i}(\alpha)\rangle)$ attains its

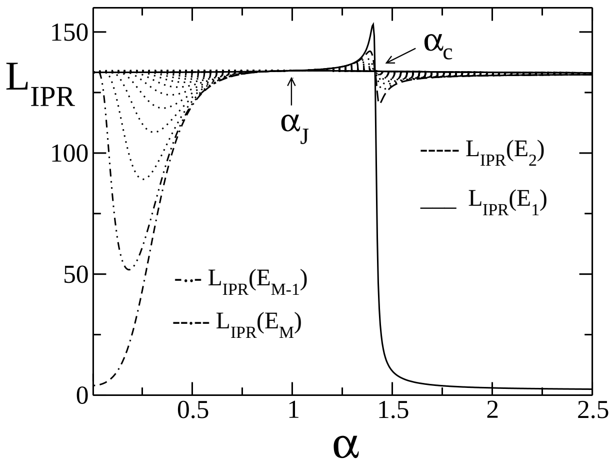

FIG. 4: The IPR ($L_{IPR} = \sum_i |\Psi_i|^2 / \sum_i |\Psi_i|^4$) of different one excitation eigen-states *vs* α, for spin chain with $N = 200$. The values of α_J and α_c are shown. For $\alpha >> \alpha_c$, the curves of the IPR for the all eigen-states, except those corresponding to the minimal and maximal eigen-energies, collapse into a single curve. For $\alpha > \alpha_c$ the curves with $L_{IPR} \sim 1$ correspond to the minimal and maximal eigen-energy states. The steep behavior of these curves when $\alpha \to \alpha_c^+$ shows the change from well localized to extended states. The localized states, with low IPR, that appear for $\alpha < \alpha_c$ correspond to states with eigen-energies near the center of the band. Near $\alpha = 0$ there are several localized states. Each curve is double as explained in the text.

minimun, the numerical results show that $\alpha^m_{E_N} < \alpha^m_{E_{N-1}} < ...$, *i.e.* the state is more localized as it is closer to $E = 0$. Besides, the number of localized states increase with N as can be seen comparing Figures 4 and 5, which correspond to $N = 200$ and $N = 40$ respectively.

For values of α larger than α_c, but very close to this value, the states become more localized, while at α_c they are all equally localized. Conversely, for values of α smaller than α_c, but very close to this value, the states become more extended than at α_c. The size of the interval around α_c in which this behavior can be observed depends on the size of the chain (compare Figures 4 and 5). The peaks of IPR observed for $\alpha < \alpha_c$ become sharper when N grows.

In the interval $\alpha > \alpha_c$ there are only two eigenstates highly localized, they correspond to the minimal and maximal eigen-energies, E_1 and E_N, the other states are extended through $N - 1$ sites of the chain.

Summarizing, it is clear that an eigen-state changes its localization when its eigen-energy

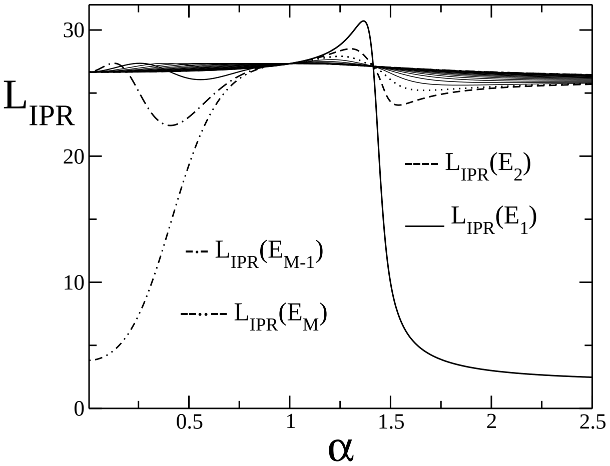

FIG. 5: The IPR of different one excitation eigen-states *vs* α, for spin chain with $N = 40$. The changes around α_c are not as pronounced as in the chain with $N = 200$ spins, compare with Figure 4.

changes as a function of α. The localization changes in the region around α_c because there the spectrum has the avoided crossings previously described.

While the IPR is useful to evaluate how much extended or localized is a state, it is a very limited tool as we will show below. In the case of a chain with only one impurity the states inside the band are very similar to the states of the homogeneous chain, *i.e.* they are wave-like superpositions of the one excitation basis set $|n\rangle$, the coefficients of the superpositions are given by Eq. 5 with θ real. For $\alpha > \alpha_c$ the minimal eigen-energy state is quite different, the coefficients of the superposition Ψ_i corresponding to $|\Psi_{E_1}\rangle$ decay exponentially, see Figure 6. The Figure 6 shows the coefficients Ψ_i for $|\Psi_{E_1}(\alpha)\rangle$ (for $\alpha = 1.6$) and $|\Psi_{E_M}(\alpha)\rangle$ (for $\alpha = 0.1$). Despite of their very different behavior both states are equally localized if the measure of localization is the IPR, effectively $L_{IPR}(\Psi_{E_1}) = L_{IPR}(\Psi_{E_M}) \simeq 5.6$ for the states whose coefficients are shown in Figure 6. This indicates that the IPR can not distinguish the exponentially localized state from the state with a wave-like superposition extended over the chain if the latter has its coefficient Ψ_1 large enough.

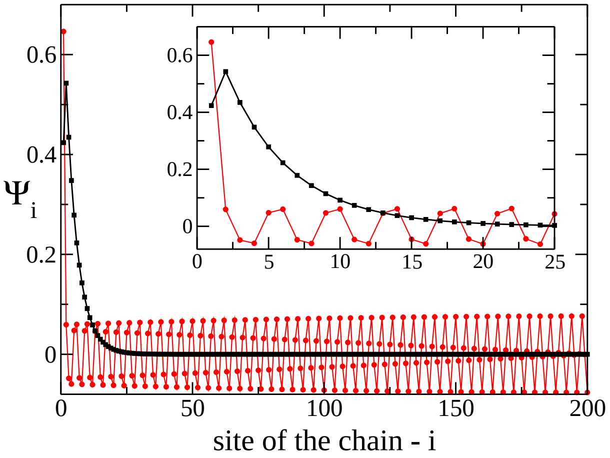

FIG. 6: (color online) The coefficients Ψ_i for two different eigenstates, $|\Psi_{E_1}(\alpha)\rangle$ for $\alpha = 1.6$ (black squares) and $|\Psi_{E_M}(\alpha)\rangle$ for $\alpha = 0.075$ (red circles). The lines are included as a guide to the eye. The states and the values of α were chosen to obtain equal values for their inverse participarion ratios.The inset shows a zoom of the region near $i = 1$

V. ENTANGLEMENT

The bipartite entanglement between two qubits can be calculated using the Concurrence [20] . The Concurrence of two qubits in an arbitrary state characterized by the density matrix ρ is given by

$$C(\rho) = max\{0, \lambda_1 - \lambda_2 - \lambda_3 - \lambda_4\}, \tag{10}$$

where the λ_i are the square roots of the eigenvalues, in decreasing order, of the non-Hermitian matrix $\rho\widetilde{\rho}$. The spin-flipped state $\widetilde{\rho}$ is defined as

$$\widetilde{\rho} = (\sigma^y \otimes \sigma^y)\rho^*(\sigma^y \otimes \sigma^y), \tag{11}$$

were ρ^* is the complex conjugate of ρ and it is taken in the computational basis, which for a pair spin-$\frac{1}{2}$ particles is $\{| \uparrow\uparrow\rangle, | \uparrow\downarrow\rangle \; | \downarrow\uparrow\rangle, | \downarrow\downarrow\rangle\}$. The concurrence takes values between 0 and 1, where 0 means that the state is disentangled whereas 1 means a maximally entangled state.

When considering a subsystem of two qubits on the chain, the concurrence is calculated with the reduced density matrix. The reduced density matrix for the spin pair (i, j), $\rho_E^{(i,j)}(\alpha)$, corresponding to the eigen-state $|\Psi_E(\alpha)\rangle$ is given by

$$\rho_E^{(i,j)}(\alpha) = \mathrm{tr}\, |\Psi_E(\alpha)\rangle \langle \Psi_E(\alpha)| = \mathrm{tr}\hat{\rho}_E(\alpha), \tag{12}$$

where the trace is taken over $N-2$ spins, those different from i and j, so $\rho_E^{(i,j)}(\alpha)$ is a 4×4 matrix.

The structure of the reduced density matrix follows from the symmetry properties of the Hamiltonian. Thus, in our case the concurrence $C(\rho^{(i,j)})$ depends on i and j, *i.e.* the indexes of the sites where the spin pair lies. Note that in the translationally invariant case $C(\rho^{(i,j)})$ depends only on $|i-j|$. In what follows $C_{i,j} = C(\rho^{(i,j)})$.

Using the definition $\langle \hat{A}\rangle = Tr(\hat{\rho}\hat{A})$, we can express all the matrix elements of the density matrix $\rho^{(i,j)}$ in terms of different spin-spin correlation functions, in particular, for nearest neighbors spins and eigenstate $|\Psi_{E_j}\rangle$, we get

$$\rho_{E_j}^{(i,i+1)} = \begin{pmatrix} a_j & 0 & 0 & 0 \\ 0 & b_j & \langle \sigma_i^+\sigma_{i+1}^-\rangle_{E_j} & 0 \\ 0 & \langle \sigma_i^+\sigma_{i+1}^-\rangle_{E_j}^* & d_j & 0 \\ 0 & 0 & 0 & 0 \end{pmatrix}, \tag{13}$$

where

$$a_j = \frac{1}{4}\langle (\sigma^z + I)_i (\sigma^z + I)_{i+1}\rangle_{E_j}, \tag{14}$$

$$b_j = \frac{1}{4}\langle (\sigma^z + I)_i (I - \sigma^z)_{i+1}\rangle_{E_j}, \tag{15}$$

$$d_j = \frac{1}{4}\langle (I - \sigma^z)_i (\sigma^z + I)_{i+1}\rangle_{E_j}, \tag{16}$$

I is the 2×2 identity matrix, $\sigma_i^{\pm} = (\sigma_i^x \pm i\sigma_i^y)/2$, and

$$\langle \ldots \rangle_{E_j} = \left\langle \Psi_{E_j} \right| \ldots \left| \Psi_{E_j} \right\rangle. \tag{17}$$

Thus, the concurrence results to be

$$C_{i,i+1}(\rho_{E_j}) = \max\{0, 4 \mid \langle \sigma_i^+\sigma_{i+1}^-\rangle_{E_j} \mid \sqrt{|b_j c_j|}\}. \tag{18}$$

Using the Hellmann-Feynman theorem, and the symmetry properties of the Hamiltonian, we find that

$$\frac{\partial E_j}{\partial \alpha} = 2J \left\langle \Psi_{E_j} \right| \sigma_1^+\sigma_2^- \left| \Psi_{E_j} \right\rangle. \tag{19}$$

From the expression for the reduced density matrix $\rho^{(i,i+1)}$, Eq. 13, it is clear that when $\langle \sigma_i^+ \sigma_{i+1}^- \rangle = 0$ the reduced density matrix is diagonal and the bipartite entanglement is zero. Moreover, from Eq. 19, when $\frac{\partial E_j}{\partial \alpha} = 0$ we have that $C_{12}(\rho_{E_j}) = 0$.

For the set of eigenstates that we are considering, the expression for the concurrence can be further simplified. It can be shown that

$$b_j = (\Psi_{i+1}^{(j)})^2, \quad c_j = (\Psi_i^{(j)})^2. \tag{20}$$

So, the concurrence for the first two spins in the eigenstate $|\Psi_{E_j}\rangle$ is given by

$$C_{12} = \max\left\{0, \left|\frac{1}{2J}\frac{\partial E_j}{\partial \alpha}(\Psi_2^{(j)})(\Psi_1^{(j)})\right|\right\}. \tag{21}$$

Note that the eigen-states are not degenerate $\forall \alpha \neq 0$, so it is equivalent to refer to a given state with eigen-energy E_i using the eigen-vector $|\Psi_{E_i}\rangle$ or the density matrix $\hat{\rho}_{E_i} = |\Psi_{E_i}\rangle\langle\Psi_{E_i}|$. The concurrence of the spin pair (i, j) when the system is in the eigen-state E_i is denoted by $C_{i,j}(\rho_{E_i})$ (we have dropped the superscript (i, j) for shortness).

We are interested in the relationship between localization and entanglement for the whole one spin excitation spectrum. We start analyzing what happens with the bipartite entanglement of the minimal eigen-energy state, E_1. According to Figure 4, the minimal eigen-energy state is strongly localized for large enough values of α. This state becomes more extended for $\alpha < \alpha_c$.

We calculated the concurrence between the first and second spins $C_{1,2}$, *i.e.* the impurity site and its nearest neighbor site, as a function of α for the minimal eigen-energy state. Figure 7 shows the behavior of $C_{1,2}(\rho_{E_1})$ as a function of α. The results shown in Figure 7 are consistent with our findings for the IPR of the minimal eigen-energy state: for large enough α ($\alpha >> \alpha_c$) the state consists in an entangled pair formed by the two first spins almost disentangled from the rest of the chain. When $\alpha \to \alpha_c^+$ the concurrence $C_{1,2} \to 0$.

Using Equations 9 and 21, it is straightforward to obtain that

$$C_{12}(\rho_{E_j}) = C_{12}(\rho_{E_{N-j+1}}), \quad j = 1, \ldots, N/2, \tag{22}$$

since that for eigenstates with symmetrical eigen-energies respect to zero we have that

$$\frac{\partial E_j}{\partial \alpha} = -\frac{\partial E_{N-j+1}}{\partial \alpha}. \tag{23}$$

The results presented until this point can be summarized as follows: the eigen-states corresponding to the minimal and maximal eigenvalues present $C_{12} \neq 0$ for $\alpha > \alpha_c$, while

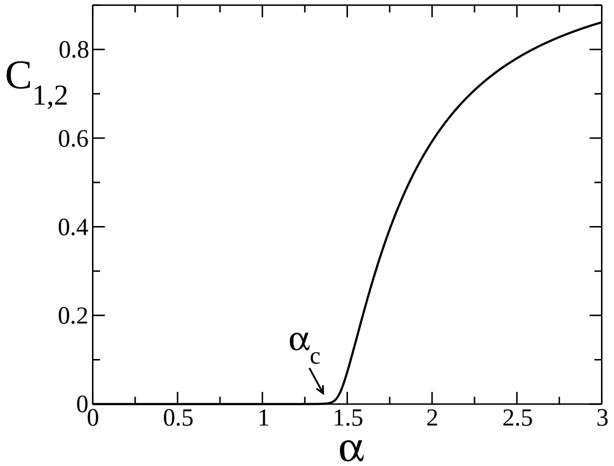

FIG. 7: The entanglement shared between the first spin (the impurity site) and and its nearest neighbor, measured by $C_{1,2}(\rho_{E_1})$ *vs* α. When the state is localized, $\alpha > \alpha_c$, it is entangled too. At the critical point, and for $\alpha \leq \alpha_c$ $C_{1,2}(\rho_{E_1}) = 0$ consistenly with $\frac{\partial E_1}{\partial \alpha} = 0$ for $\alpha \leq \alpha_c$.

the states inside the band have $C_{12} \neq 0$ basically for $\alpha < \alpha_c$, more precisely, as functions of $C_{1,2}(\rho_{E_1}(\alpha))$ and $C_{1,2}(\rho_{E_N}(\alpha))$ present their maximun value for $\alpha > \alpha_c$, while $C_{1,2}(\rho_{E_i}(\alpha))$ presents its maximum for $\alpha < \alpha_c$, if $i \neq 1$,or N.

As mentioned above, when the minimal (or maximal) eigenvalue enters into the band there is a number of avoided crossings in the spectrum and the localization of the different eigenstates involved in those avoided crossings changes. So it makes sense to take a look at the behavior of C_{12} for the eigenstates with energies close to E_1 in the region of $\alpha \lesssim \alpha_c$. Figure 8 shows the concurrence C_{12} for a few eigenstates.

The behavior of the curves shown in Figure 8 suggests a way to order the eigen-states through the position of the peaks of each curve. Calling α_i^m to the abscissa where $C_{12}(\rho_{E_i}(\alpha))$ has its maximun, then $\alpha_2^m > ... > \alpha_N^m$. A similar scenario can be observed in the behavior of the concurrence of the eigenstates near the top of the band when the maximal eigen-energy comes into the band.

Because bipartite entanglement is a local quantity while IPR is global, it is natural to ask about the behavior of the bipartite entanglement of other pairs of spins and what features of C_{12} remain or not when looking at some pair of spins $(i, i+1)$. We choose to study C_{23}, *i.e.* the first pair on the chain that does not include the impurity site. Figure 9 shows the behavior of C_{23} for the minimal eigen-energy state and for other few eigenstates.

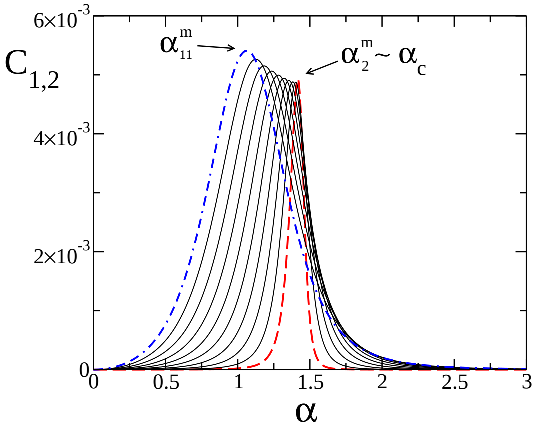

FIG. 8: (color online) $C_{12}(\rho_{E_i}(\alpha))$ *vs* α, for $i = 2, 3, \ldots, 11$. The results were obtained for a chain of $M = 40$ spins. Each curve $C_{12}(\rho_{E_i}(\alpha))$ has a single peak. The peaks are ordered by eigen-energy, the rightmost peak corresponds to $C_{12}(\rho_{E_2}(\alpha))$ (red dashed line), the peak to its left corresponds to $C_{12}(\rho_{E_3}(\alpha))$, and so on. The leftmost peak corresponds to the curve with the highest eigen-energy shown in the figure, E_{11} (blue dashed-dotted line).

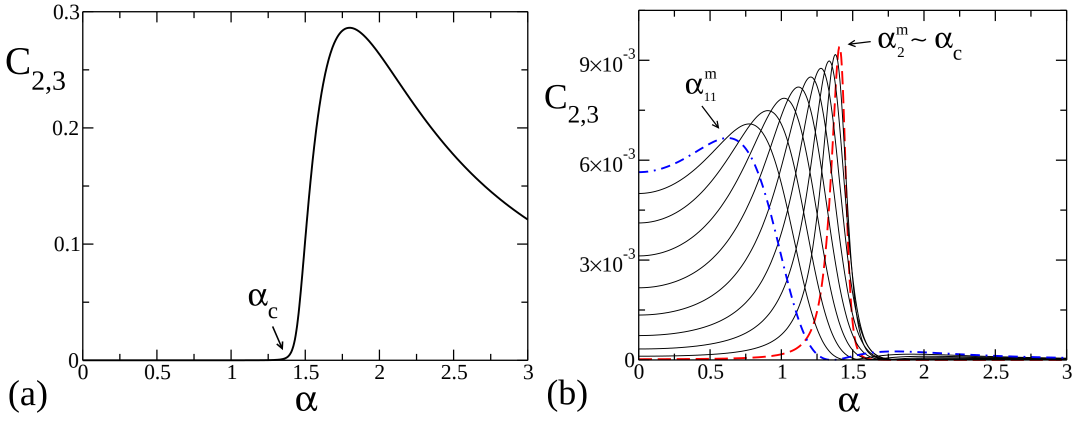

FIG. 9: (color online) $C_{2,3}$ *vs* α for a spin chain with $N = 40$. (a) $C_{2,3}(\rho_{E_1})$ *vs* α. (b) $C_{2,3}(\rho_{E_i})$, $i = 2, 3, \ldots 11$, each curve has a single maximun, the leftmost peak corresponds to $C_{2,3}(\rho_{E_2})$ (red dashed line) and the rightmost to $C_{2,3}(\rho_{E_{11}})$ (blue dashed-dotted line) .

The behavior of $C_{2,3}(\rho_{E_1}(\alpha))$, as shown in Figure 9, is quite similar to the behavior of $C_{1,2}(\rho_{E_1}(\alpha))$, compare with Figure 7. Both concurrences give, more or less, the same information: the eigenstate has (bipartite) entanglement for $\alpha > \alpha_c$, and the (bipartite) entanglement is zero for $\alpha \leq \alpha_c$. Each curve $C_{1,2}(\rho_{E_i}(\alpha))$ has a single maximun. Again, it is possible to order the eigenstates accordingly with its entanglement, calling α_i^m the abscissa where $C_{23}(\rho_{E_i}(\alpha))$ has its maximun, then again $\alpha_2^m > ... > \alpha_N^m$, however it must be noted that the ordinate of the peaks decreases when the eigen-energy of the state grows.

VI. DISCUSSION

Except for the states $|\Psi_1\rangle$ and $|\Psi_N\rangle$ in the region where their eigenvalues are isolated from the band, the one spin excitation eigenstates are weakly entangled. For $\alpha > \alpha_c$ the minimal eigen-energy state can be written as $|\Psi_1\rangle = \sum_i \Psi_i^{(1)}|i\rangle$, where the coefficientes $\Psi_i^{(1)}$ decay exponentially for $i \geq 2$. Actually, all the eigenstates inside the band can be approximated by the eigenstates of the homogeneous problem with wave-like coefficients as in Eq. 5, but for the Ψ_1 coefficient. The coefficient Ψ_1 behaves differently because of the presence of the impurity.

When $|\Psi_1\rangle$ is localized, $\alpha > \alpha_c$, $\Psi_1^{(1)} \lesssim \Psi_2^{(1)}$. Instead, when a state inside the band is localized, say $|\Psi_{E_j}\rangle$, $\Psi_1^{(j)} > \Psi_2^{(j)}$, and the coefficients with $n \geq 2$ are roughly given by $\Psi_n^{(j)} \simeq de^{i\theta n} + d'e^{-i\theta n} \sim \mathcal{O}(1/\sqrt{N})$ (see Figure 6, and Eq. 5).

The scenario described in the previous paragraph explains, why $|\Psi_{E_1}\rangle$ and $|\Psi_{E_N}\rangle$ are the only eigenstates that carries a significant amount of entanglement for α large enough. C_{12} is proportional to i) the derivative of the eigen-energy, which is significant only for E_1 and E_N for $\alpha > \alpha_c$; ii) the coefficients Ψ_1 and Ψ_2 (Eq. 21). In the case of a exponentially localized state, for example $|\Psi_{E_1}(\alpha = 2)\rangle$, the first two coefficients are such that $\Psi_1^{(1)} \simeq \Psi_2^{(1)}$. For a state $|\Psi_{E_j}\rangle$, belonging to the band, the derivative of the energy is small **and** $\Psi_i^{(j)} \sim 1/\sqrt{N}$ $(i > 1)$ which results in a very small value for C_{12}. From Figure 3, $|dE_j/d\alpha| < 0.3$, $\Psi_i^{(j)} \sim 1/\sqrt{200}$ and $\Psi_1^{(j)} \sim 0.6$. Collecting these values, we get $C_{12} < 7 \times 10^{-3}$ for a typical state inside the band, which is in excellent agreement with the results shown in Figure 8.

The argument in the previos paragraph explains why two eigenstates with similar inverse participation ratio, $|\Psi_{E_1}\rangle$ for $\alpha > \alpha_c$ and $|\Psi_{E_M}\rangle$ for $\alpha \simeq 0$, do not have similar entanglement, the former has $\Psi_1^{(1)} \simeq \Psi_2^{(1)}$ and the latter has $\Psi_2^{(E_M)} \simeq 1/\sqrt{N}$.

The set of one excitation eigentates, of the chain with one impurity, possess only one eigenstate that carries a significant amount of entanglement could has inmediate consequences if the chain were to be used to transfer entanglement from one extreme of the chain to the other. Since the only eigenstate with significant entanglement is located at the impurity it seems that it is necessary to locate impurities at both extremes of the chain in order to successfully transfer entanglement. This is consistent with the findings of Plastina and Apollaro in [21].

There is enough evidence to affirm that the entanglement of quantum states whose eigen-energies present avoided crossings will show steep changes near of them ([18],[22], this work). In our case there is a number of avoided crossings that appears between succesive levels, when E_1 comes into the band as α decreases from values larger than the critical. The avoided crossing between E_1 and E_2 is nearer to α_c than the avoided crossing between E_2 and E_3, and so on. This is the behavior depicted in Fig. 8. The width of the peak in C_{12} of a given state (see Fig. 8) is related to the magnitude of the derivative of the eigen-energy of the state, the peak is sharper for $C_{12}(\rho_{E_2})$ and the succesive peaks are more and more rounded.

While IPR is an appealing quantity since it is very easy to calculate, we have shown that it is not possible to guess how much entanglement has a given state. Moreover, we have shown that IPR is not always useful to determine localization. The examples analyzed show that based on the IPR it is not possible to guess how much entanglement has a given state, anyway it remains an appealing quantity since it is very easy to calculate. There is not, to our knowledge, a simple quantity that allows to relate, in a direct way, localization and entanglement. This subject will be object of further investigation.

Acknowledgments

We would like to acknowledge SECYT-UNC 05/B337, CONICET PIP 112-200801-01741, and FONCyT Grant N^o PICT-2005 33305 (Argentina) for partial financial support of this work. We thank B. Franzoni and G. A. Alvarez for helpful discussions and critical reading of the manuscript.

---

[1] Valerie Coffman, Joydip Kundu, and William K. Wootters, Phys. Rev. A **61**, 052306 (2000)

[2] Kevin M. O'Connor and William K. Wootters, Phys. Rev. A **63**, 052302 (2001)

[3] S. Michalakis and B. Nachtergaele, Phys. Rev Lett. **97**,140601 (2006)

[4] Omar Osenda, Zhen Huang, and Sabre Kais, Phys. Rev. A **67**, 062321 (2003)

[5] H.-J. Sommers and K. Zyczkowski, J. Phys. A **37**, 8457 (2004); O. Giraud, *ibid.* **40**, 2793 (2007); M. Znidaric, *ibid.* **40**, F105 (2007).

[6] Tony J.G. Apollaro and Francesco Plastina, Open Sys. and Information Dyn. **14**, 41 (2007).

[7] Tony J. G. Apollaro and Francesco Plastina, Phys. Rev. A **74**,062316 (2006).

[8] B. Georgeot and D. L. Shepelyansky, Phys. Rev. E **62**, 3504(2000); 62, 6366 (2000).

[9] D. A. Meyer and N. R. Wallach, J. Math. Phys. **43**, 4273 (2002).

[10] O. Giraud, J. Martin, and B. Georgeot, Phys. Rev. A **76**, 042333 (2007).

[11] Lorenza Viola and Winton G Brown, J. Phys. A: Math. Theor. **40**, 8109 (2007).

[12] Haibin Li, XiaoGuang Wang and Bambi Hu, J. Phys. A: Math. Gen. **37**, 10665 (2004)

[13] Xun Jia, Arvind R. Subramaniam, Ilya A. Gruzberg, and Sudip Chakravarty, Phys Rev. B **77**, 014208 (2008)

[14] Haibin Li and XiaoGuang Wang, Modern Physics Letters B **19**, 517 (2005).

[15] I.L. Chuang, L.M.K. Vandersypen, X. Zhou, D.B. Leung, and S. Lloyd, Nature (London) **393**, 143 (1998)

[16] Y. Makhlin, G. Schön, and A Shnirman, Rev. Mod. Phys. **73**, 357 (2001)

[17] L.F. Santos and M.I. Dyckman, Phys. Rev B **68**, 214410 (2003).

[18] Alejandro Ferrón, Omar Osenda, and Pablo Serra, Phys. Rev. A **79**, 032509 (2009)

[19] E. Lieb, T. Schultz, and D. Mattis, Ann. Phys. N.Y. **16**, 407 (1961)

[20] W. K. Wootters, Phys. Rev. Lett. **80**, 2245 (1998).

[21] F. Plastina and T. J. G. Apollaro, Phys. Rev. Lett. **99**, 177210 (2007)

[22] R. Gonzlez-Frez and J. S. Dehesa, Phys. Rev. Lett. **91**, 113001 (2003)